

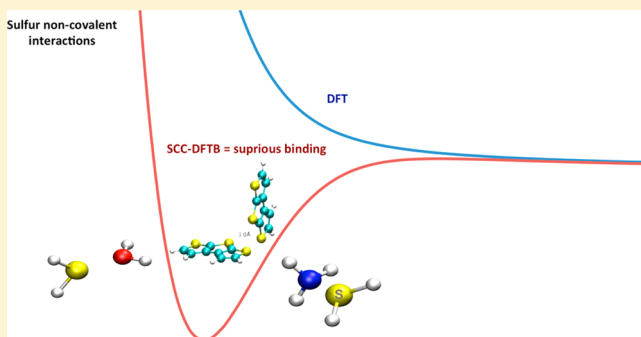
A Caveat on SCC-DFTB and Noncovalent Interactions Involving Sulfur Atoms

Riccardo Petraglia and Clemence Corminboeuf*

Laboratory for Computational Molecular Design, Institut des Sciences et Ingénierie Chimiques, Ecole Polytechnique Fédérale de Lausanne, CH-1015 Lausanne, Switzerland

S Supporting Information

ABSTRACT: Accurate modeling of noncovalent interactions involving sulfur today is ubiquitous, particularly with regard to the role played by sulfur-containing heterocycles in the field of organic electronics. The density functional tight binding (DFTB) method offers a good compromise between computational efficiency and accuracy, enabling the treatment of thousands of atoms at a fraction of the cost of density functional theory (DFT) evaluations. DFTB is an approximate quantum chemical approach that is based on the DFT total energy expression. Here, we address a critical issue inherent to the DFTB parametrization, which prevents the use of the DFTB framework for simulating noncovalent interactions involving sulfur atoms and precludes its combination with a dispersion correction.^{1–5} Dramatic examples of structural patterns relevant to the field of organic electronics illustrate that DFTB delivers erroneous (i.e., qualitatively wrong) results involving spurious binding.



INTRODUCTION

Noncovalent interactions play key roles in many areas of chemistry, including being of crucial importance for self-assembly and molecular recognition processes. More specifically, interactions involving sulfur-containing heterocycles currently receive significant interest due to their primary role in the field of organic electronics. For example, aggregation between oligothiophene chains provides the core functionality that makes plastic electronics an attractive and viable alternative to traditional silicon analogs.^{6–12} In petroleum chemistry, the situation is reversed as these same dispersion forces are detrimental: thiophenes are a key component of asphaltenes, where their interaction leads to increased oil viscosity that alters oil upgrading,^{13,14} rather than providing functionality. Noncovalent interactions involving sulfur atoms are also significant in the biochemical world,^{6,14,15} where, for instance, sulfur- π interactions assist in forming protein tertiary structures.^{15–19}

The computational analysis of organic electronics suffers from two main challenges; the first involves modeling of nanoscale oligothiophene assemblies themselves (e.g., what are the structural characteristics? Figure 1²⁰). The second challenge is providing a reliable characterization of electronic properties and functions.^{21–24} In principle, these structural and electronic aspects could be addressed conjointly using the density functional theory framework;²⁵ however, quantum descriptions of systems of this size remain prohibitive due to computational cost. Thus, the development and application of more approximate schemes that enable the treatment of thousands of atoms are indispensable.^{1,26} The density functional tight

binding²⁷ (DFTB) approach (especially in its SCC-DFTB²⁸ and DFTB3^{29,30} variants *—vide infra*), based on DFT, can simulate large systems²⁶ with reasonable accuracy^{31–33} and provide a majority of electronic structure related properties. Like DFT, DFTB suffers from several shortcomings, including unreliable descriptions of long-range intermolecular interactions. However, it is now quite clear that this particular shortfall can be overcome using *a posteriori* dispersion corrections.^{1–5}

In principle, the DFTB scheme can be applied to investigate organic electronic materials featuring noncovalent interactions between sulfur atoms,^{34–40} when combined with a dispersion correction.^{1–5} Unfortunately, as demonstrated here, DFTB suffers from a major qualitative drawback that affects both geometries and energies of noncovalent interactions and ultimately leads to completely erroneous data any time sulfur atoms are present. In this paper, we provide a brief overview of the DFTB scheme, prior to illustrating a few alarming examples of this DFTB flaw.

DFTB IN A NUTSHELL

This section overviews the original density functional tight-binding scheme and its more recent variants^{27–30} and provides the necessary theoretical basis for understanding the source of the “sulfur problem.” It is not meant to be a detailed description of DFTB, which is the subject of several excellent

Received: April 12, 2013

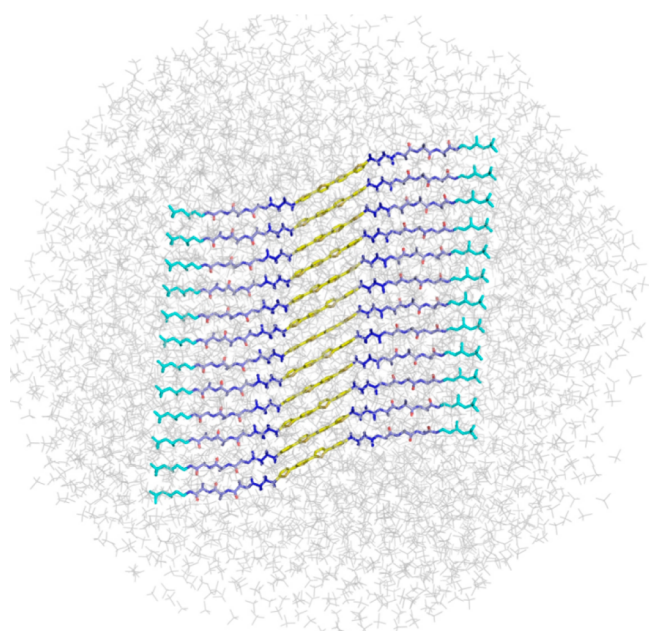


Figure 1. A recent example of hierarchically structured microfibers of a “single stack” quaterthiophene (yellow) nanowire.²⁰ The oligopeptide-substituted quaterthiophenes benefit from a synergistic enhancement of hydrogen-bonding and π - π interactions that are important for electronic applications. The computational description of such assemblies relies upon the proper evaluation of noncovalent interactions.

articles.^{28,28,30,33,41–43} Akin to tight binding models,²⁷ the total energy in DFTB is expressed as²⁷

$$E = E_{\text{el}} + E_{\text{rep}} = \sum_{i=1}^M \varepsilon_i + \frac{1}{2} \sum_{\alpha\beta}^N V(R_{\alpha\beta}) \quad (1)$$

where ε_i are eigenvalues of a Schrodinger-like equation and $V(R_{\alpha\beta})$ is a short-range pairwise repulsion between atoms that depends exclusively on the interatomic distance.

The electronic terms, given as E_{el} , differ among the DFTB variants, in the description of hydrogen bond properties and the charge transfer between bonding atoms. The self-consistent charge density functional tight-binding scheme, developed by Elstner and co-workers,²⁸ accounts for the charge transfer between bonded atoms, which is absent in the NCC-DFTB²⁷ (Not-Charge-Consistent-DFTB) approach. The Self-Consistent-Charge DFTB approach (SCC-DFTB)²⁸ enables the description not only of solid state materials but also more complex systems such as biological macromolecules and nanosystems.³⁹ The most recent DFTB3,^{29,30} improves performance for systems in which atoms carry significant partial charges.⁴⁴

The electronic term in DFTB3 is defined as follows

$$\begin{aligned} E_{\text{el}} &= E_{\text{NCC}} + E_{\text{SCC}} + E_{3\text{rd}} \\ &= \sum_i^M \sum_{\alpha\beta}^N \sum_{\mu \in \alpha} \sum_{\nu \in \beta} c_{\mu} c_{\nu} H_{\mu\nu}^0 + \frac{1}{2} \sum_{\alpha\beta}^N \Delta q_{\alpha} \Delta q_{\beta} \gamma_{\alpha\beta} \\ &\quad + \frac{1}{3} \sum_{\alpha\beta}^N \Delta q_{\alpha}^2 \Delta q_{\beta} \Gamma_{\alpha\beta} \end{aligned} \quad (2)$$

where N is the number of atoms in the system, α and β are atom indexes, and M is the number of occupied molecular one-

electron orbitals i that are expanded within the LCAO ansatz using a suitable set of constrained atomic orbitals

$$\psi_i(\mathbf{r}) = \sum_{\nu} c_{\nu i} \phi_{\nu}(\mathbf{r} - \mathbf{R}_{\alpha}) \quad (3)$$

These constrained atomic orbitals are determined by solving a modified set of Schrodinger equations for free neutral pseudoatoms

$$\left[\mathcal{T} + V_{\text{nuc}} + V_{\text{H}} + V_{\text{xc}} + \left(\frac{r}{r^{\text{wf}}} \right)^2 \right] \phi_{\nu} = \varepsilon_i \phi_{\nu} \quad (4)$$

The first three terms of the equation are the kinetic energy, the nuclear repulsive potential, and the Hartree potential, respectively. V_{xc} is the exchange-correlation potential that, generally, is expressed as the PBE XC potential.^{45,46} r^{wf} is the wave function compression radius that is taken as twice the covalent radius (e.g., for sulfur, $r^{\text{wf}} = 2 \text{ \AA} = 2r^{\text{cov}}$). The Hamiltonian matrix elements are written in a two-center approximation as

$$\mathcal{H}_{\mu\nu}^0 = \begin{cases} \varepsilon^{\text{freeatom}} & \text{if } \alpha = \beta, \mu = \nu \\ \langle \phi_{\mu}^{\alpha} | \mathcal{T} + V[\rho_{\alpha}^0 + \rho_{\beta}^0] | \phi_{\nu}^{\beta} \rangle & \text{if } \alpha \neq \beta, \mu \neq \nu \\ 0 & \text{if } \alpha = \beta, \mu \neq \nu \end{cases} \quad (5)$$

The $\varepsilon^{\text{freeatom}}$'s are computed neglecting the extra term (r/r^{wf}) in eq 4 so that this formulation of $\mathcal{H}_{\mu\nu}^0$ ensures the correct limit for free atoms. ρ_i^0 represents free atom compressed densities computed using eq 4 by substituting r^{wf} with r^{dens} . Whereas the densities were originally determined directly from the compressed wave functions, the use of alternative constrained radii (generally larger, e.g., 4.76 Å for sulfur) has been shown to improve results (see ref 29 and reference cited therein). The choice of r^{dens} is not trivial but is known to be critical for obtaining good energies.²⁷ In order to reduce computational demand, the Hamiltonian and overlap matrix elements are precomputed using a minimal basis set and tabulated for different distances in a Slater–Koster approach.⁴⁷ Using compressed wave functions and densities improves the portability of these parameters.²⁸

The DFTB approach is made self-consistent by improving the NCC-DFTB scheme with²⁸

$$E_{\text{SCC}} = \frac{1}{2} \sum_{\alpha\beta}^N \Delta q_{\alpha} \Delta q_{\beta} \gamma_{\alpha\beta} \quad (6)$$

where Δq_i is the charge difference with respect to the neutral state with density ρ_i^0 and $\gamma_{\alpha\beta}$ is a function describing the interactions between non-neutral atoms α and β . γ is chosen such that at large interatomic distances E_{SCC} tends to a pure Coulombic interaction energy between charges Δq_i .²⁸ $\gamma_{\alpha\alpha}$ is approximated as the difference between the ionization potential and the electron affinity of the free atom. This difference is related to the chemical hardness or to the Hubbard parameters (U); hence $\gamma_{\alpha\beta}$ is approximated as a function of U_{ω} , U_{β} , and $R_{\alpha\beta}$ even at medium distances.²⁸ To improve the descriptions of hydrogen bonds, a suitable repulsive term is added to $\gamma_{\alpha\beta}$ at covalent distances when one of the atoms involved is hydrogen.²⁹ Since Δq_i are computed with the Mulliken scheme, where the charge depends on the coefficients c_{μ} and c_{ν} , the SCC-DFTB scheme is self-consistent.²⁸

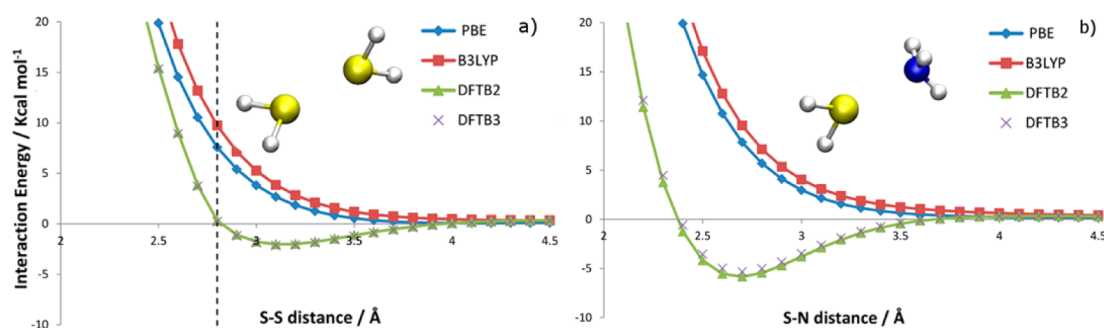


Figure 2. Interaction energy profiles of the H_2S dimer (left) and of H_2S with NH_3 (right) at the DFT and DFTB levels. The SCC-DFTB and DFTB3 computations were performed using the MIO parameters. DFT energies are computed at the PBE/6-31G* and B3LYP/6-31G* levels. The vertical dashed line indicates the cutoff of the spline in the sulfur–sulfur interaction repulsive term. Note that the H_2S dimer does not bind in the absence of a dispersion correction to DFT approximations.

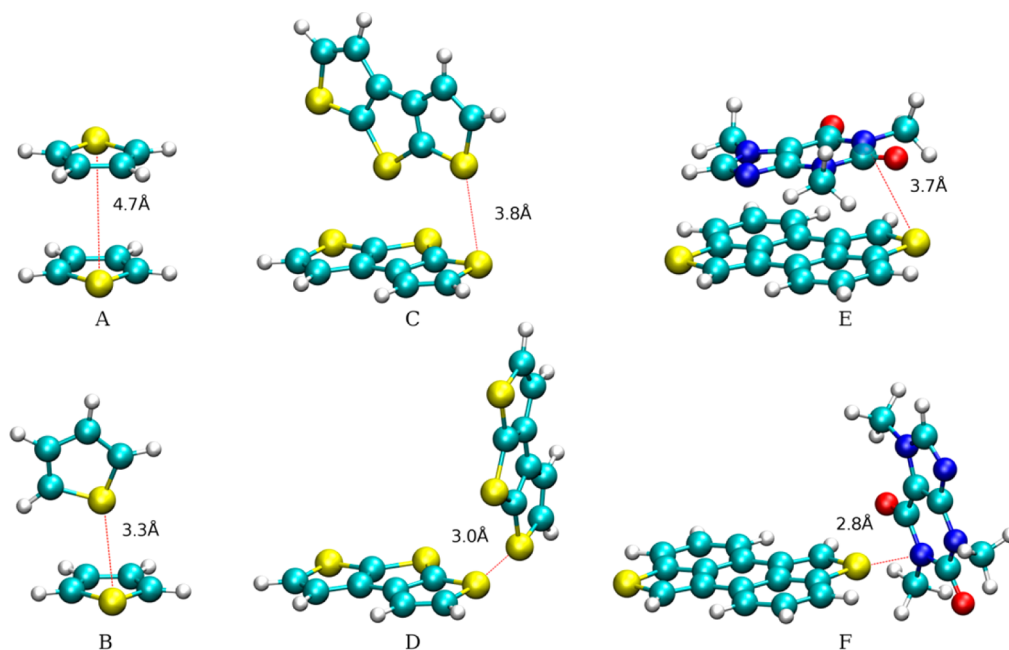


Figure 3. The reference geometry of the antiparallel thiophene dimer (A)⁶² and the DFTB3 optimized geometry (B) using the MIO set of parameters. The T-shape annelated β -triophene dimer optimized at the PBE0-dDsC/def2-SVP level (C)⁶¹ and at the DFTB3 level (D). A recent example of caffeine sensing optimized at the PBE0-dDsC/def2-SVP level (E)⁶⁵ and at the DFTB3 level (F).

Considering the Hubbard parameter independent from the atomic charge is a severe limitation.^{48,49} To improve the description of systems with large intermolecular charge transfer, the following “third order” term is introduced:^{29,30}

$$E_{3\text{rd}} = \frac{1}{3} \sum_{\alpha\beta}^N \Delta q_{\alpha}^2 \Delta q_{\beta} \Gamma_{\alpha\beta} \quad (7)$$

where the Hubbard parameters depend on Δq_i through the function $\Gamma_{\alpha\beta}$. Hubbard parameters needed in SCC-DFTB, here, are replaced by their derivative with respect to the charge. In practice, this term is a correction on the energy that accounts for the dependence on atomic charges of the Hubbard parameters.

The repulsive term accounts for all approximations made in the electronic part. In practice, $V(R_{\alpha\beta})$ is a spline^{30,33} (or polynomial²⁸) function fit to the difference in energies between DFT (usually the B3LYP functional) and the electronic term of DFTB at various bond lengths²⁸ for an appropriate, usually small,^{28,30,33,48} set of molecules.

None of the DFTB variants are considered as “semi-empirical” in the sense that the parameters are not fitted to experimental data: some (such as the Hubbard parameters and derivatives) are obtained directly from DFT computations while others (such as the repulsive potential) are fitted to DFT results.^{28,33,48,49} This makes DFTB a DFT-based approximation, affected by the same deficiencies as DFT (vide infra).

COMPUTATIONAL DETAILS

All SCC-DFTB²⁸ and DFTB3^{29,30} computations were performed using the MIO/NHorg^{28,50} parameter set in the DFTB+ release 1.2.²⁶ DFTB3 computations used the *calc* parameters from Gaus et al.³⁰ The DFTB geometry optimizations were performed at the DFTB3 level using default settings. DFT computations were performed in MOLPRO at the PBE/6-31G*^{45,46,51} or B3LYP/6-31G*^{51–55} levels using default thresholds and grids.

■ CRITICAL FAILURE OF SULFUR AT DFTB LEVEL

The DFTB description of sulfur-containing compounds relies upon a few critical aspects within the parametrization: the electronic terms in the existing MIO^{28,50} parameters are based on DFT computations using the PBE exchange-correlation functional. The proper description of hypervalent species is achieved by inclusion of d orbitals in the minimal basis set. The repulsive potential is fitted to various bond lengths for a small set of seven sulfur-containing molecules (see Niehaus et al.⁵⁰ for further details). Given that the parametrization is based on PBE and B3LYP DFT computations, DFTB results will be compared with values from B3LYP/def2-TZVP and PBE/def2-TZVP, referred to herein as “DFT level”. Note that since neither standard DFT approximations nor DFTB account for dispersion interactions, the energy profiles of van der Waals complexes are generally expected to be repulsive even though some functional approximations (e.g., PBE,^{45,46} TPSS⁵⁶) can bind rare-gas dimers and other noncovalently bound diatomics without a dispersion correction.^{57–60}

Figure 2a shows DFT and DFTB energy profiles along the S–S intermolecular distance for two hydrosulfuric acid molecules, where the sulfur atoms point toward one another. To our surprise, the SCC-DFTB profile is attractive and thus qualitatively wrong; it does not parallel the repulsive DFT curves. Instead, a binding region with a maximum value of about 2 kcal/mol^{−1} is found between 2.8 and 4.0 Å, which potentially leads to serious consequences (vide infra) in, for instance, molecular dynamic simulations. The shortcomings illustrated by Figure 2 persist in more complex systems, including the antiparallel thiophene dimer and a T-shape dimer of annelated β -trithiophenes⁶¹ (Figure 3). Comparisons of the antiparallel thiophene dimer reference geometries computed by Steinmann et al.,⁶² Figure 3A, and by the nondispersion corrected DFTB3 level (Figure 3B) show a decrease in the S–S distance from 4.66 Å to 3.27 Å. The latter distance is significantly shorter than the accurate S–S equilibrium distance, and the final geometry is spurious. At the DFT levels, the overall intermolecular interaction is repulsive, and as one expects, the two molecules move away from one another if no dispersion correction is utilized. Invoking a dispersion correction in the DFT optimization of the thiophene dimer maintains the antiparallel configuration (that is a local minimum⁶²), which can be attributed to favorable π -interactions. Figure 3C displays the optimized geometry at the PBE0-dDsC/def2-SVP level of a T-shape dimer of annelated β -trithiophenes. Geometry optimization at the DFTB3 level (without dispersion correction) causes the S–S distance to decrease from 3.84 Å (3C) to 3.02 Å (3D). At the noncorrected DFT levels, the overall intermolecular interaction is again repulsive. Clearly, the DFTB3 optimization is dominated by the “wrong” S–S attractive potential, which negatively impacts the description of any stacked oligothiophenes or more complex systems, such as those given in Figure 3. This shortcoming is specific to sulfur atoms as the noncovalent interaction involving other heavy atoms is repulsive at the DFTB level (see e.g., Figure S1 for the DFTB profile of the water dimer).

These same drawbacks affect energy profiles of systems that contain noncovalent interactions between sulfur and any other atoms, e.g., H, N, C, and O. As an example, Figure 2b shows the contrasting DFT and DFTB interaction energy profile along the S–N distance for an ammonia/hydrosulfuric acid

dimer where the nitrogen and sulfur atoms point toward one another. The maximum binding energy in the DFTB profile is located at ~ 2.7 Å and corresponds to a stabilization of 5.9 kcal mol^{−1}, while the expected profile, given by the two density functionals, is repulsive at all distances! Note that DFTB3 exhibits the same behavior as SCC-DFTB and that the problem is limited only to noncovalent interactions.⁵⁰ These findings are preliminary indications that “the sulfur problem” arises from the parametrization (only one set of parameters is currently available for sulfur)⁵⁰ and not from a defect of the SCC-DFTB theory.

A related example includes the improper description of the π – π -stacking interactions between caffeine and a novel chemosensor recently designed by Corminboeuf et al.⁶³ and synthesized by Severin et al.⁶⁴ Figure 3 shows the resulting DFTB3 geometry optimization of the caffeine-dye complex (Figure 3F) starting from the PBE0-dDsC/def2-SVP⁶⁵ geometry (Figure 3E): the S–N distance in the reference structure is significantly longer (3.67 Å) than that given by DFTB3 (2.83 Å). As mentioned before, the expected behavior is for the two molecules to move apart from each other. Note that the shortest S–N distances in the caffeine-dye complex optimized at the DFTB3 level closely match the spurious 2.7 Å equilibrium energy distance of the S–N DFTB profiles (Figure 2). Obviously, spurious S–N overbinding drives the geometry optimization of the caffeine-dye complex toward the incorrect structure.

Providing a quick fix to the problem is not straightforward. In addition, the inclusion or parametrization of a proper *a posteriori* dispersion correction to DFTB is irrelevant, since this would only increase the observed overbinding. One possible solution considered was modification of the repulsive term $V(R_{\alpha\beta})$ to increase the repulsion between the sulfur and the other atoms in order to prevent the noncovalent overbinding. Similar modifications of the repulsive terms have been utilized in the past to correct for the N–H binding energy in a specific environment, but only small compensations were needed in that case.^{33,66} To correct for the error of the sulfur noncovalent interaction, $V(R_{\alpha\beta})$ must be radically modified: the cutoff of the repulsive term is never larger than 2.8 Å (see Figure 2) in the original parameters, while it must be extended to about 4.0 Å, depending on the atom pair, to overcome the error in the electronic term. This type of modification contrasts with the principle on which the repulsive term is based: $V(R_{\alpha\beta})$ must be strictly pairwise, short-range, and repulsive.^{28,67,68} Short range implies that the cutoff of the repulsive term should be only slightly longer than a covalent bond length, to make it strictly pairwise. Despite this conceptual challenge, we attempted reparameterization by fitting the repulsive term to the difference between the DFT–B3LYP/def2-TZVP total energy and SCC-DFTB electronic energy at various distances for one representative molecular system for each parameter (e.g., two H₂S molecules arranged in the Figure 2 conformation were used for the S–S repulsive parameter). Note that we fitted the intermolecular energies instead of the covalent bond energies as done by Niehaus et al.⁵⁰ Using this approach, the intramolecular properties were not significantly affected (see Table S1), but the resulting energy profiles for noncovalent interactions did not transfer to larger molecules (see Figures S2 and S3).

An alternative approach circumventing the problem was using a brute force simplex algorithm that modifies the cubic splines associated with $V(R_{SS})$ and $V(R_{SC})$ to fit an ensemble of

DFTB to DFT profiles. Even in this case, the results were not satisfactory, as the final DFTB values remained qualitatively different from DFT (Table S2).

Our efforts indicate that modifying the repulsive term is insufficient to fix the “sulfur problem” discussed here. Recently, a new set of parameters for hydrogen and second row nonmetal elements was developed,³³ herein it was found that the wave function compression radii (r^{wf}) affect noncovalent bond distances. In particular a large r^{wf} causes an increase in Pauli repulsion and therefore a larger noncovalent bond distance. Our examination of the influence of r^{wf} values on the interaction energy (see Figure S4) seems to confirm that a larger r^{wf} could lead to less attractive profiles and that reparameterization of the electronic term is the only way toward fixing the spurious interactions involving sulfur atoms.

CONCLUSION

SCC-DFTB and DFTB3 approaches can lead to highly valuable insights and unravel complex problems involving large molecular systems. Further development and validation of such methods could be strongly beneficial for the design of organic based functional nanostructures. Unfortunately, we demonstrate here that the DFTB geometries of sulfur-containing compounds featuring noncovalent interactions are unreliable, and often result in dramatic qualitative failures preventing the use of all DFTB variants in geometry optimization and, more importantly, in molecular dynamic simulations. Thus, to successfully apply DFTB approaches to supramolecular systems containing sulfur, a revision of the DFTB parameters is urgent. Attempts to correct this “sulfur problem” by adding a correction within the repulsive energy were unsuccessful. Our analysis indicates that only a complete revision of the electronic parametrization term will render the DFTB framework reliable for simulations of sulfur containing compounds. We have also suggested that larger wave function compression radii could solve the problem. The DFTB community should be cautioned from using the existing sulfur parameters, especially if the sulfur noncovalent interactions are the key factors in determining a complex's geometry, and hope that this work will stimulate the development of new parameters.

ASSOCIATED CONTENT

Supporting Information

The data associated with the energy profiles, the geometry coordinates and the test on the parametrization are given. This information is available free of charge via the Internet at <http://pubs.acs.org>.

AUTHOR INFORMATION

Corresponding Author

*E-mail: clemence.corminboeuf@epfl.ch.

Notes

The authors declare no competing financial interest.

ACKNOWLEDGMENTS

C.C. acknowledges the Swiss NSF Grant 200021_121577/1, ERC starting grant 306528, and EPFL for financial support. The authors thank Dr. Matthew Wodrich and Jerome Gonthier for insightful discussions and Shanshan Wu for Figure 1.

REFERENCES

- (1) Elstner, M.; Hobza, P.; Frauenheim, T.; Suhai, S.; Kaxiras, E. *J. Chem. Phys.* **2001**, *114*, 5149–5155.
- (2) Wu, X.; Vargas, M. C.; Nayak, S.; Lotrich, V.; Scoles, G. *J. Chem. Phys.* **2001**, *115*, 8748–8757.
- (3) Meijer, E. J.; Sprik, M. *J. Chem. Phys.* **1996**, *105*, 8684–8689.
- (4) Řezáč, J.; Hobza, P. *J. Chem. Theory Comput.* **2011**, *8*, 141–151.
- (5) Zhechkov, L.; Heine, T.; Patchkovskii, S.; Seifert, G.; Duarte, H. A. *J. Chem. Theory Comput.* **2005**, *1*, 841–847.
- (6) Facchetti, A. *Chem. Mater.* **2011**, *23*, 733–758.
- (7) Vondrak, T.; Wang, H.; Winget, P.; Cramer, C. J.; Zhu, X.-Y. *J. Am. Chem. Soc.* **2000**, *122*, 4700–4707.
- (8) Shaw, J. M.; Seidler, P. F. *IBM J. Res. Dev.* **2001**, *45*, 3–9.
- (9) Saito, G. *Phosphorus Sulfur Silicon Relat. Elem.* **1992**, *67*, 345–360.
- (10) Kelley, T. W.; Baude, P. F.; Gerlach, C.; Ender, D. E.; Muyres, D.; Haase, M. A.; Vogel, D. E.; Theiss, S. D. *Chem. Mater.* **2004**, *16*, 4413–4422.
- (11) Hamed, M.; Forchheimer, R.; Inganäs, O. *Nat. Mater.* **2007**, *6*, 357–362.
- (12) Günes, S.; Neugebauer, H.; Sariciftci, N. S. *Chem. Rev.* **2007**, *107*, 1324–1338.
- (13) Murgich, J.; Abanero, J. A.; Strausz, O. P. *Energy Fuels* **1999**, *13*, 278–286.
- (14) Mackie, I. D.; McClure, S. A.; DiLabio, G. A. *J. Phys. Chem. A* **2009**, *113*, 5476–5484.
- (15) Tauer, T. P.; Derrick, M. E.; Sherrill, C. D. *J. Phys. Chem. A* **2005**, *109*, 191–196.
- (16) Reid, K. S. C.; Lindley, P. F.; Thornton, J. M. *FEBS Lett.* **1985**, *190*, 209–213.
- (17) Morgan, R. S.; Tatsch, C. E.; Gushard, R. H.; McAdon, J. M.; Warme, P. K. *Int. J. Pept. Protein Res.* **1978**, *11*, 209–217.
- (18) Zauhar, R. J.; Colbert, C. L.; Morgan, R. S.; Welsh, W. J. *Biopolymers* **2000**, *53*, 233–248.
- (19) Morgan, R. S.; McAdon, J. M. *Int. J. Pept. Protein Res.* **1980**, *15*, 177–180.
- (20) Spitzner, E. C.; Feifer, M.; Magerle, R.; Steinmann, N. S.; Corminboeuf, C.; Frauenrath, H. *ACS Nano* **2013**, submitted.
- (21) Bredas, J. L.; Silbey, R.; Boudreaux, D. S.; Chance, R. R. *J. Am. Chem. Soc.* **1983**, *105*, 6555–6559.
- (22) Cornil, J.; Beljonne, D.; Calbert, J.-P.; Brédas, J.-L. *Adv. Mater.* **2001**, *13*, 1053–1067.
- (23) Newman, C. R.; Frisbie, C. D.; da Silva Filho, D. A.; Brédas, J.-L.; Ewbank, P. C.; Mann, K. R. *Chem. Mater.* **2004**, *16*, 4436–4451.
- (24) Grimm, B.; Risko, C.; Azoulay, J. D.; Brédas, J.-L.; Bazan, G. C. *Chem. Sci.* **2013**, *4*, 1807–1819.
- (25) Kohn, W.; Sham, L. J. *Phys. Rev.* **1965**, *140*, A1133–A1138.
- (26) Aradi, B.; Hourahine, B.; Frauenheim, T. *J. Phys. Chem. A* **2007**, *111*, 5678–5684.
- (27) Foulkes, W. M. C.; Haydock, R. *Phys. Rev. B* **1989**, *39*, 12520–12536.
- (28) Elstner, M.; Porezag, D.; Jungnickel, G.; Elsner, J.; Haugk, M.; Frauenheim, T.; Suhai, S.; Seifert, G. *Phys. Rev. B* **1998**, *58*, 7260–7268.
- (29) Yang, Y. H.; York, D.; Cui, Q.; Elstner, M. *J. Phys. Chem.* **2007**, *111*, 10861–10873.
- (30) Gaus, M.; Cui, Q.; Elstner, M. *J. Chem. Theory Comput.* **2011**, *7*, 931–948.
- (31) Korth, M.; Thiel, W. *J. Chem. Theory Comput.* **2011**, *7*, 2929–2936.
- (32) Zheng, G.; Irle, S.; Morokuma, K. *Chem. Phys. Lett.* **2005**, *412*, 210–216.
- (33) Gaus, M.; Goetz, A.; Elstner, M. *J. Chem. Theory Comput.* **2013**, *9*, 338–354.
- (34) Elstner, M.; Frauenheim, T.; Kaxiras, E.; Seifert, G.; Suhai, S. *Phys. Status Solidi B* **2000**, *217*, 357–376.
- (35) Cui, Q.; Elstner, M.; Kaxiras, E.; Frauenheim, T.; Karplus, M. *J. Phys. Chem. B* **2001**, *105*, 569–585.
- (36) McNamara, J. P.; Hillier, I. H. *Phys. Chem. Chem. Phys.* **2007**, *9*, 2362–2370.

- (37) Page, A. J.; Ohta, Y.; Okamoto, Y.; Irle, S.; Morokuma, K. *J. Phys. Chem. C* **2009**, *113*, 20198–20207.
- (38) Page, A. J.; Ohta, Y.; Irle, S.; Morokuma, K. *Acc. Chem. Res.* **2010**, *43*, 1375–1385.
- (39) Zhukovskii, Y. F.; Piskunov, S.; Bellucci, S. *Nanosci. Nanotechnol. Lett.* **2012**, *4*, 1074–1081.
- (40) Welke, K.; Watanabe, H. C.; Wolter, T.; Gaus, M.; Elstner, M. *Phys. Chem. Chem. Phys.* **2013**, submitted.
- (41) Seifert, G. *J. Phys. Chem. A* **2007**, *111*, 5609–5613.
- (42) Seifert, G.; Joswig, J.-O. *Wiley Interdiscip. Rev. Comput. Mol. Sci.* **2012**, *2*, 456–465.
- (43) Porezag, D.; Frauenheim, T.; Köhler, T.; Seifert, G.; Kaschner, R. *Phys. Rev. B* **1995**, *51*, 12947–12957.
- (44) Barone, V.; Carnimeo, I.; Scalmani, G. *J. Chem. Theory Comput.* **2013**, submitted.
- (45) Perdew, J. P.; Burke, K.; Ernzerhof, M. *Phys. Rev. Lett.* **1996**, *77*, 3865–3868.
- (46) Perdew, J. P.; Burke, K.; Ernzerhof, M. *Phys. Rev. Lett.* **1997**, *78*, 1396–1396.
- (47) Slater, J. C.; Koster, G. F. *Phys. Rev.* **1954**, *94*, 1498–1524.
- (48) Elstner, M. *Theor. Chem. Acc.* **2006**, *116*, 316–325.
- (49) Elstner, M. *J. Phys. Chem. A* **2007**, *111*, 5614–5621.
- (50) Niehaus, T. A.; Elstner, M.; Frauenheim, T.; Suhai, S. *J. Mol. Struct.: THEOCHEM* **2001**, *541*, 185–194.
- (51) Pople, J. J. *J. Chem. Phys.* **1975**, *62*, 2921.
- (52) Lee, C.; Yang, W.; Parr, R. G. *Phys. Rev. B* **1988**, *37*, 785–789.
- (53) Becke, A. D. *Phys. Rev.* **1988**, *38*, 3098–3100.
- (54) Becke, A. D. *J. Chem. Phys.* **1993**, *98*, 5648–5652.
- (55) Stephens, P. J.; Devlin, F. J.; Chabalowski, C. F.; Frisch, M. J. *J. Phys. Chem.* **1994**, *98*, 11623–11627.
- (56) Tao, J.; Perdew, J. P.; Staroverov, V. N.; Scuseria, G. E. *Phys. Rev. Lett.* **2003**, *91*, 146401.
- (57) Ruzsinszky, A.; Perdew, J. P.; Csonka, G. I. *J. Phys. Chem. A* **2005**, *109*, 11015–11021.
- (58) Patton, D. C.; Pederson, M. R. *Phys. Rev.* **1997**, *56*, R2495–R2498.
- (59) Tao, J.; Perdew, J. P. *J. Chem. Phys.* **2005**, *122*, 114102–114109.
- (60) Zhang, Y.; Pan, W.; Yang, W. *J. Chem. Phys.* **1997**, *107*, 7921–7925.
- (61) Liu, H.; Kang, S.; Lee, J. Y. *J. Phys. Chem. B* **2011**, *115*, 5113–5120.
- (62) Steinmann, S. N.; Corminboeuf, C. *J. Chem. Theory Comput.* **2012**, *8*, 4305–4316.
- (63) Rochat, S.; Steinmann, S. N.; Corminboeuf, C.; Severin, K. *Chem. Commun.* **2011**, *47*, 10584–10586.
- (64) Luisier, N.; Ruggi, A.; Steinmann, S. N.; Favre, L.; Gaeng, N.; Corminboeuf, C.; Severin, K. *Org. Biomol. Chem.* **2012**, *10*, 7487–7490.
- (65) Gonthier, J. F.; Steinmann, S. N.; Roch, L.; Ruggi, A.; Luisier, N.; Severin, K.; Corminboeuf, C. *Chem. Commun.* **2012**, *48*, 9239–9241.
- (66) Bondar, A.-N.; Fischer, S.; Smith, J. C.; Elstner, M.; Suhai, S. *J. Am. Chem. Soc.* **2004**, *126*, 14668–14677.
- (67) Gaus, M.; Chou, C.-P.; Witek, H.; Elstner, M. *J. Phys. Chem. A* **2009**, *113*, 11866–11881.
- (68) Kaminski, S.; Giese, T.; Gaus, M.; York, D. M.; Elstner, M. *J. Phys. Chem. A* **2012**, 9131–9141.